Journal of Molecular Liquids 312 (2020) 113475

Contents lists available at ScienceDirect

Journal of Molecular Liquids

journal homepage: www.elsevier.com/locate/molliq

Intensified elimination of aqueous heavy metal ions using chicken feathers chemically modified by a batch method

Rupa Chakraborty [a], Anupama Asthana [a], Ajaya Kumar Singh [a,*], Sushma Yadav [a], Md. Abu Bin Hasan Susan [b], Sónia A.C. Carabineiro [c]

[a] Department of Chemistry, Govt. V. Y. T. PG. Autonomous College, Durg, 491001, Chhattisgarh, India
[b] Department of Chemistry, University of Dhaka, Dhaka 1000, Bangladesh
[c] LAQV-REQUIMTE, Department of Chemistry, NOVA School of Science and Technology, Universidade NOVA de Lisboa, 2829-516 Caparica, Portugal

ARTICLE INFO

Article history:
Received 24 February 2020
Received in revised form 16 May 2020
Accepted 27 May 2020
Available online 29 May 2020

Keywords:
Heavy metal ions
Modified chicken feathers
Adsorption isotherm
Kinetics
Thermodynamics
Regeneration

ABSTRACT

Modified chicken feathers (MCFs) were used as adsorbents for the removal of Co(II), Cu(II), Fe(II) and Ni(II) heavy metal ions from water by varying pH, adsorbent concentration and time. MCFs were characterized using Fourier Transform Infrared (FTIR) spectroscopy, Scanning Electron Microscopic (SEM) analysis, Energy Dispersive X-ray (EDX) spectroscopy, Adsorption of N_2 at −196 °C, Thermogravimetric analysis (TGA) and X-ray Diffraction (XRD) analysis. The adsorption isotherm for the metal ions could be well explained by the Langmuir model. The maximum adsorption capacities were 200.0, 50.0, 43.47, and 4.85 mg/g, following the sequence: Cu(II) > Co(II) > Fe(II) > Ni(II), respectively. Removal efficiencies of Co(II), Cu(II), Fe(II) and Ni(II) ions were 98.7%, 98.9%, 98.7% and 99%, respectively, for 20 mg/L concentration. The study of the adsorption kinetics for metal ions on MCFs confirmed that the process followed a pseudo second order kinetic model in all cases. The thermodynamics showed that the adsorption processes for metal ions adsorption on MCFs were spontaneous and endothermic. MCFs exhibited a good recyclability and high adsorption efficacy after 7 cycles using a 0.1 M EDTA solution, maintaining 90% of the adsorption ability.

1. Introduction

Many industries produce toxic wastewaters containing heavy metals and such pollution is a major problem. Mercury, arsenic, cadmium, lead, chromium, copper, nickel and cobalt are very toxic heavy metals with harmful effects [1,2]. Even low concentrations of such ions cause damages to the environment and public health, as they are non-biodegradable and highly toxic. The majority of heavy metals present in wastewater come from pesticides, fertilizers, metals present in paints, pigments, textile industries, chemical industries and battery manufacturing [3]. Copper (II), cobalt (II), iron (II) and nickel (II) are common examples of heavy metal ions commonly found in industrial wastewater.

Copper is a micronutrient essential to humans but higher concentrations of this metal, continually ingested, can have harmful effects on humans, such as Alzheimer's and Wilson diseases, liver and kidney damage, insomnia, vomiting, diarrhoea and lung cancer [4,5].The maximum limit allowed for Cu set by the American Environmental Protection Agency (EPA) for drinking water is 1.3 mg/L [6].

Cobalt is an essential dietary component to humans but is also toxic and dangerous at higher concentrations [7]. It can be found at the wastewaters of nuclear power plants and is used in various industrial applications. Severe cobalt poisoning may cause serious human health problems, such as allergic dermatitis, rhinitis, asthma, heart damage and heart failure [8].

Iron is also an essential element, with extreme importance in oxygen transportation and storage (in the forms of haemoglobin and myoglobin, both containing Fe(II) ions [9]). However, Fe can be present in high concentrations in effluents from industry, namely from steel tempering, mining and coal. The intake of high amounts of iron can cause various health problems, such as stomach pain, nausea and vomiting; in higher concentrations, cancer and fatal damages to the brain and liver.

Nickel is also toxic at higher concentrations, being found in chemical industries, electroplating, mining, refining, paints and ink formulation units [10]. Nickel can lead to a skin disease called nickel-eczema and other adverse health effects, such as nausea, chronic asthma, coughing and cancer. EPA set the maximum allowed level of nickel for drinking water as 0.015 mg/L [11].

Several techniques, including physical and chemical processes, were reported for the elimination of heavy metal ions, namely, chemical precipitation, ion exchange, adsorption, reverse osmosis, etc. [12–15].

* Corresponding author.
E-mail address: ajayaksingh_au@yahoo.co.in (A.K. Singh).

https://doi.org/10.1016/j.molliq.2020.113475
0167-7322/© 2020 Published by Elsevier B.V.

These methods involve high costs and disposal problems of the resulting sludge. In contrast, the adsorption process shows various economical and environmental benefits, and has been the best technique for removing heavy metal ions.

Nowadays, carbon materials, such as activated carbon [16], carbon nanotubes [17], graphene oxide nanoparticles [18,19] and nanocomposite [20] are extensively used as adsorbents due to their high adsorption capacity. However, their cost is very high and thus their uses are limited. Therefore, it is imperative to explore easily available and cheaper alternatives. Bio-wastes can be used as adsorbents given their low cost, abundance, high sorption capacity, eco-friendliness, and ease of operation [21]. Several publications report the use of low cost bio-wastes, like modified corncob [22], apricot shell [23], sugarcane bagasse [24], saw dust [25], litchi peel [26], Sterculia guttata shell [27] and *Swietenia mahagoni* shells [28]. These materials contain cellulose, lignin, and hemicelluloses with several functional groups, like carbonyl, hydroxyl and amino, that are able to form bonds with heavy metals [29].

In a recent study, we used animal waste material, i.e., chicken feathers (CFs), which are abundantly available in poultry processing plants. CFs contains keratin protein (nearly 90–91%) with several amino acids with a large amount of cysteine [30]. Keratin contains carboxylic (–COOH), hydroxyl (−OH), amino ($-NH_2$) and thiol (−SH) groups, that can form bonds with heavy metal ions. The application of chicken feathers as adsorbents showed good results in the adsorption of heavy metal ions, dyes and other organic toxic compounds [31,32].

The aim of this work is to use modified chicken feathers (MCFs) as adsorbents for soluble heavy metal ions (Cu^{2+}, Co^{2+}, $Fe^{2+}$and Ni^{2+}) from water. The adsorption process was tested using a batch method by varying different parameters, like pH, temperature, contact time and adsorbent dosage. Several techniques were used for the characterization of MCFs, and to understand the adsorption results. Studies of adsorption kinetics, isotherm and thermodynamic were carried out and analyzed in detail. The ultimate goal has been to elucidate adsorption mechanism by MCFs for the heavy metal ions.

2. Experimental

2.1. Materials and reagents

Copper sulphate ($CuSO_4 \cdot 5H_2O$), cobalt nitrate ($CoNO_3 \cdot 6H_2O$), ferrous ammonium sulphate $(NH_4)_2Fe(SO_4)_2 \cdot 6H_2O$ potassium thiocyanate, nickel sulphate ($NiSO_4 \cdot 5H_2O$), hydrochloric acid (HCl), sodium hydroxide (NaOH), hydroxyl amine hydroxide and ammonia solution were procured from CDH (Mumbai, India). Sodium diethyl dithiocarbamate, dimethylglyoxime and 1,10-phenanthrolene were purchased from HIMEDIA (Mumbai, India). The chemicals were analytical grade. Solutions were prepared using double distilled water. Stock solutions of Cu^{2+}, Co^{2+}, Fe^{2+} and Ni^{2+} (1000 mg/L) were prepared by dissolution of a proper amount of analytical grade $CuSO_4 \cdot 5H_2O$, $CoNO_3 \cdot 6H_2O$ and $(NH_4)_2Fe(SO_4)_2$, $NiSO_4 \cdot 5H_2O$ in water. Other concentrations were prepared by systematic dilution of the main stock solution.

2.2. Preparation of the adsorbent

Raw chicken feathers (RCFs) were collected from a local poultry farm, washed with detergent and tap water, and then rinsed with distilled water several times. CFs were dipped into aqueous ethanol (20% v/v) for 12 h for totally cleaning rachis and barbs (shown in Fig. 1(a)) from organic residues and later rinsed with double distilled water and dried. After drying, the rachis was removed and the barbs were cut into small pieces (as seen in Fig. 1(b)) with the help of scissors. Then 2% aqueous NaOH solution (100 mL) and 4.0 mL ethylenediamine were added to CFs (4.0 g) in a 250 mL beaker. The sample was kept for 2 h at room temperature. After modification, CFs were washed several times with double distilled water and dried at 100 °C. The final product is seen in Fig. 1(c).

2.3. Characterization of the adsorbent

Several characterization techniques were used to characterize the prepared adsorbent. All samples were analyzed by Fourier Transform Infrared (FTIR) spectroscopy in the 4000–400 cm^{-1} spectral wavenumber range on a Thermo Nicolet Avatar 370 FT-IR spectrophotometer. The surface morphology of MCFs was evaluated on a SEM JEOL JSM-6390 Scanning Electron Microscope. The elemental compositions of the MCFs were obtained by Energy Dispersive X-ray (EDX) spectroscopy (OXFORD XMX N). X-ray diffraction (XRD) analysis of the developed MCFs were carried out using PANalytical-X'Pert^3 powder instrument. N_2 gas adsorption-desorption analysis of MCFs were carried out on a surface area and pore analyzer (Belsorp mini II, BEL, Japan Inc) at −196 °C. Thermogravimetric analysis (TGA) was conducted with a Perkin Elmer STA 6000 TG/DT model (at 10 °C min^{-1}, from 30 to 500 °C, in N_2atmosphere). All the heavy metal ion measurements were carried out with a UV–Vis. spectrophotometer (Systronics UV–Visible spectrophometer- 117).

2.4. Batch adsorption experiments

The adsorption of Co(II), Cu(II), Fe(II) and Ni(II) ions onto MCFs was performed in 100 mL conical flasks by batch equilibrium using a water bath incubator shaker (Tempstar). In this experiment, the necessary amount of MCFs was added to each conical flask containing 10 mL of Co(II), Cu(II), Fe(II) and Ni(II), with the desired concentration. The solution pH was adjusted by drop addition of 0.1 M HCl and 0.1 M NaOH. Subsequently, the mixture was shaken on a water bath shaker for the desired time. After adsorption, the solutions were filtered and quantitative analysis of the remaining metal ion concentration was made with the help of a UV–visible spectrophotometer. The Co(II), Cu(II), Fe(II) and Ni(II) ions were determined by UV–visible spectrophotometry using sodium diethyl dithiocarbamate, potassium thiocyanate, 1,10-phenanthrolene, and dimethylglyoxime, respectively [33].

The removal percentage of metal ions was obtained by the following equation:

$$R\,(\%) = \frac{C_0 - C_e}{C_e} \times 100 \tag{1}$$

and the amount of adsorbed metal ions was calculated by:

$$q_e = \frac{C_0 - C_e}{m} \times V \tag{2}$$

where C_0 and C_e are, respectively, the initial and the equilibrium concentrations of metal ions in the solution (in mg/L), and V is the solution volume (L).

3. Results and discussion

3.1. Characterization of the adsorbents

3.1.1. Proximate and ultimate analyses

The results for proximate and ultimate analyses of MCFs are given in Table S1, which show that the sample has organic and inorganic constituents. The carbon content of MCFs is approximately 68.48% (ultimate analysis) and fixed carbon is 81.32% (proximate analysis). MCFs are characterized by a higher content of fixed carbon and low volatile matter and ash contents.

3.1.2. Textural characterization

MCFs were further investigated by N_2adsorption and desorption analysis at −196 °C, as shown in Figs. S1 and S2. The BET surface area and BJH pore size of MCFs were 16 m^2/g and 1.5 nm (Table S2).

Fig. 1. Chicken feather close-up image showing rachis and barbs (a) chicken feather barbs before (b) and after (c) modification.

3.1.3. Fourier-transform infrared (FTIR) spectrophotometric analysis

FTIR spectra (shown in Fig. 2) were obtained to analyse the functional groups in the CFs during modification and adsorption. Fig. 2 (a) depicts the FTIR spectrum of RCFs. The broad absorption band at 3398 cm^{-1} is assigned to the O—H and N—H stretching vibration. The peak at 2963 cm^{-1} is caused by the C—H stretching vibration. The band at 1643 cm^{-1} is assigned to C═N and C═O stretching vibration of amide I. The amide II band occurs at sharp bands of 1541 cm^{-1} and 1446 cm^{-1}, respectively due to the N—H bending and C—H stretching vibration. The peak around 1398 cm^{-1} corresponds to the O—H in plane bending vibration. The peak at 1248 cm^{-1} is attributed to the amide III [34,35]. The band at 1075 cm^{-1} may be caused by the C—O symmetric stretching vibration of secondary alcohol.

The FTIR spectrum of MCFs is shown in Fig. 2(b). The spectra of the MCFs were very similar to the spectrum of the RCFs, suggesting that MCFs show only a few changes in the chemical structure. After modification, the absorption band at 3398 cm^{-1} shifted to 3438 cm^{-1}. Thus, it can be concluded that the hydroxyl group participated in adsorption process. The peak shape of O—H (3438 cm^{-1}) and C—O (1062 cm^{-1}) changed after Cu^{2+}, Ni^{2+}, Co^{2+} and Fe^{2+} adsorption [Fig. 2(c)–(f)]. These changes might be attributed to interaction between the adsorbent and metal ions.

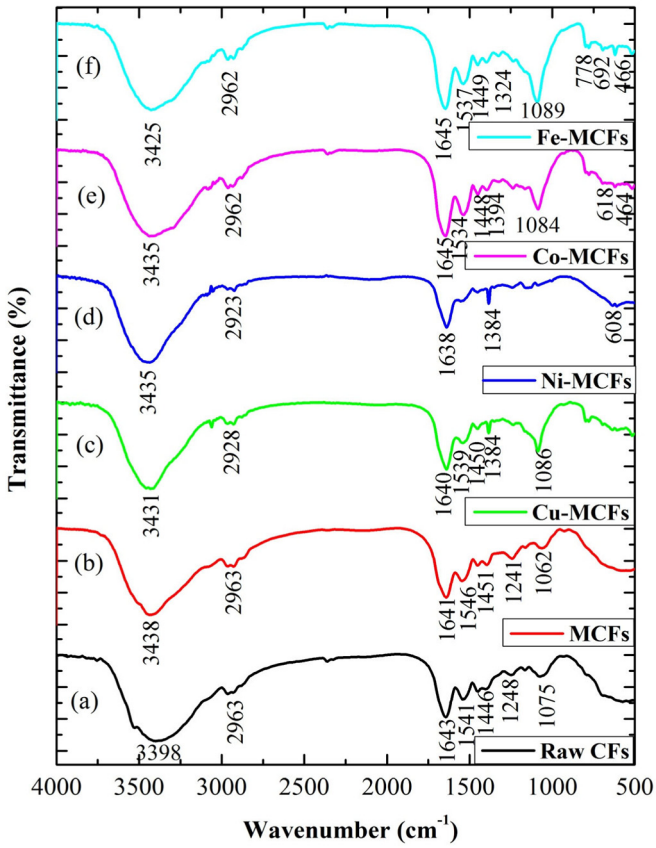

Fig. 2. FT-IR spectra of RCFs (a); MCFs (b); MCFs loaded with copper (c); nickel (d); cobalt (e) and iron (f).

3.1.4. Scanning electron microscopic (SEM) analysis

The morphology of RCFs (before modification) shows rough fibrous structure (Fig. 3a). But after modification, the surface of the MCFs shows well developed pores (Fig. 3b).

The surface of MCFs (Fig. 3b) is more rugged than the RCFs (Fig. 3a). The rough and porous surface enhances the adsorption capacity of MCFs compared to RCFs. The metal ions can be adsorbed onto the surface functional groups. After adsorption of Co(II), Cu(II), Fe(II) and Ni(II) ions, the surface morphology significantly changed, a newly bulky coated white layer of ions being formed on the surface of the MCFs (Fig. 3c, d and e).

3.1.5. Energy dispersive X-ray (EDX) spectroscopy analysis

The EDX analysis of MCFs indicates the presence of a high percentage of C, O and S and traces of Na [Fig. 4(a)]. Sodium was introduced onto the adsorbent surface in the modification process using sodium hydroxide. However, due to the intrinsic limitations of EDX analysis towards N detection (it has low photon energy), this element was not found in the spectra of MCFs shown in Fig. 4(a). Other authors were also not able to detect nitrogen in a xanthan gum samples modified with ethylenediamine [36].

Since elemental sulphur can bind to heavy metal ions, new metal ion peaks can be observed in the EDX spectra of Fig. 4(b), (c) and (d), which are not present in Fig. 4(a). Therefore, EDX analysis corroborates the adsorption of Cu(II), Ni(II), Fe(II) and Co(II) ions onto the surface of MCFs.

3.1.6. Thermal stability

The thermal stability of MCFs was assessed by thermogravimetric analysis (TGA) and the results can be found in Fig. 5. The first decrease in weight may be due to the loss of moisture (8.45%) at 100 °C. The second weight decrease at 355 °C (mass loss of ~56.85%) is due to peptide bridge and protein chain linkage thermal denaturation [37–39]. In the last step, barbs were totally decomposed (355 °C to 560 °C) with the highest weight loss (73.32%) leading to total degradation. The barbs completely degraded to its elements around 550 °C. At that temperature, the weight loss rate stabilised and a carbonised residue was left (26.68% of the original barb mass) [40]. Derivative thermogravimetry (DTG) of MCFs showed two exothermic peaks at 60 °C and 310 °C [41]. The fastest weight loss rate of 412 μg/min occurred at 310 °C [42].

3.1.7. X-ray diffraction (XRD) analysis

Fig. S3 depicts the XRD patterns of RCFs and MCFs. There is no appreciable change in the spectrum of MCFs compared to RCFs. Two broad peaks observed at 2θ around 9.3° and 19.2°, can be attributed to semi-

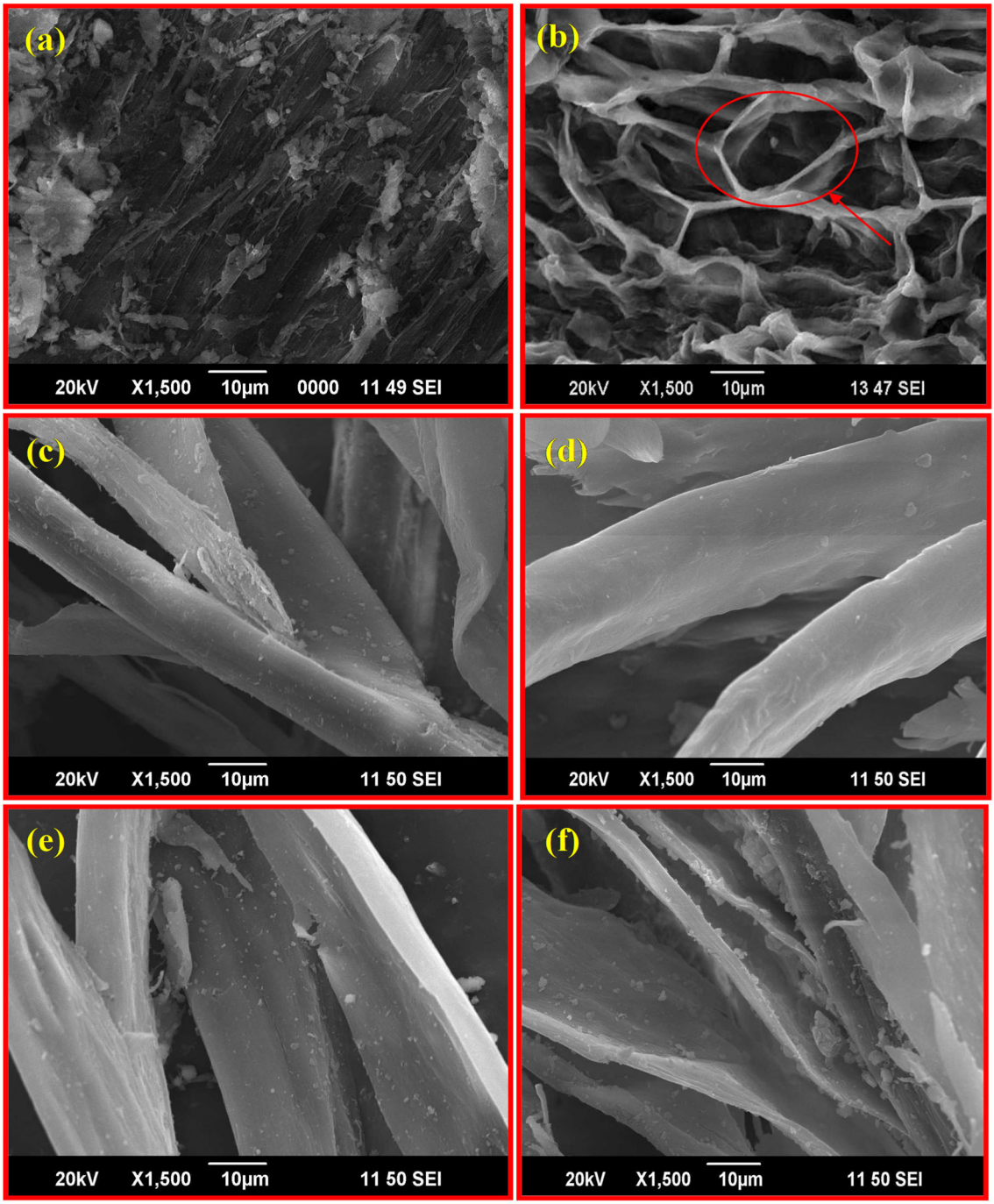

Fig. 3. Scanning electron micrographs of CFs at 1500× magnification: RCFs (a), MCFs (b), MCFs loaded with copper (c), nickel (d), cobalt (e) and iron (f).

crystalline keratin protein. The diffraction peak at $2\theta \approx 9.3°$ shows the keratin α-helix conformation, whereas the peak at $2\theta \approx 19.2°$ is indexed for the β-sheet of keratin secondary structure [Fig. S3(a) and S3(b)].

3.2. Effect of pH

The pH of the solution has a crucial effect on the adsorption of metal ions by MCFs. The FTIR results confirmed that the MCFs have a variety of surface groups, like hydroxyl, carboxyl and amine. Therefore, the pH of the solution will be influenced by such functional groups and affect the formation of bonds with the metal ions. The effect of the pH (from 2 to 9) on the elimination of the four metal ions was examined and results are found in Fig. 6.

The removal percentage shows the lowest value at pH 2.0 and reached its maximum as pH increased up to 3–4. The minimum adsorption found at low pH may be due to more protons being available in aqueous solution that are present in most of the active sites of the adsorbent surface. Thus, less metal ions are adsorbed because of the electrostatic repulsion between H^+ ions on adsorbent surface and the metal ions. Furthermore, at higher pH values (>6.0), a decrease in adsorption is found, which is due to the formation of hydroxylated (soluble) complexes of metal ions that compete with the active sites, resulting in a decrease of the removal capacity. The maximum removal efficiency of Cu

(II), Ni(II) and Co(II), that is, 98.73%, 97.66% and 97.44%, respectively, was found at pH 6.0. The amounts removed slowly decreased when the pH value increased above 6.0, as the heavy metal ions formed precipitates. The highest level of Fe(II) adsorption was observed at pH 3.0.

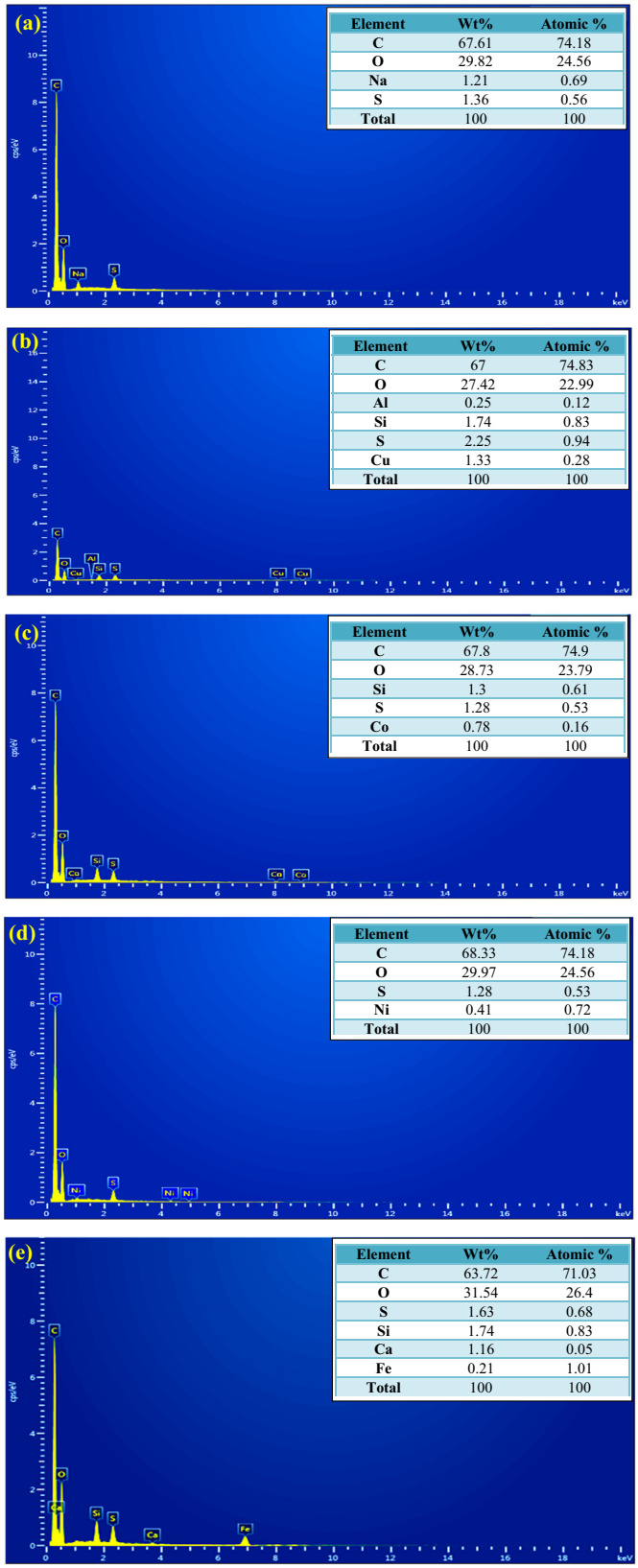

Fig. 4. EDX analysis of MCFs before adsorption (a) and MCFs after copper (b), cobalt (c), nickel (d) and iron (e) adsorption.

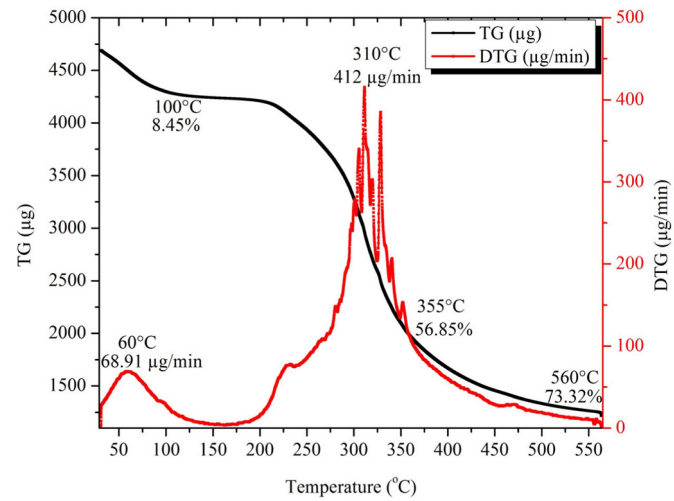

Fig. 5. TG–DTG curve of MCFs.

3.3. Effect of dosage

The effect of MCFs dosage on the removal of Co(II), Cu(II), Ni(II), and Fe(II) ions was tested and results can be found in Fig. 7. It is clear that the elimination efficiency of Co(II), Cu(II), Fe(II) and Ni(II) ions increased sharply with MCFs dose. The amount of Cu(II) removed increased from 79.3% to 98.65% when the dosage of MCFs increased from 1.0 to 9.0 g L^{-1}. Also, Ni(II) elimination increased from 26.5% to 99.95% with an increase of MCFs from 1.0 to 7.0 g L^{-1}. Co(II) removal increased from 54.35% to 96.25% when amount of MCFs increased from 1.0 to 4.0 g L^{-1} and Fe(II) removal was enhanced from 73.15% to 98.7% with an increase of MCFs from 1.0 to 9.0 g L^{-1}. However, the removal efficiency became nearly constant when the MCFs dosage exceeded 9.0 g L^{-1} for Cu(II), 4.0 g L^{-1} for Co(II), 7.0 g L^{-1} for Ni(II) and 9.0 g L^{-1} for Fe(II). It is clear that concentration of the metal ions in aqueous solution decreases when the adsorbent dosage increases, for each initial concentration of metal.

3.4. Effect of contact time and adsorption kinetics

The impact of contact time on Co(II), Cu(II), Ni(II), and Fe(II) adsorption (20 mg/L initial concentration) is depicted in Fig. 8, which shows

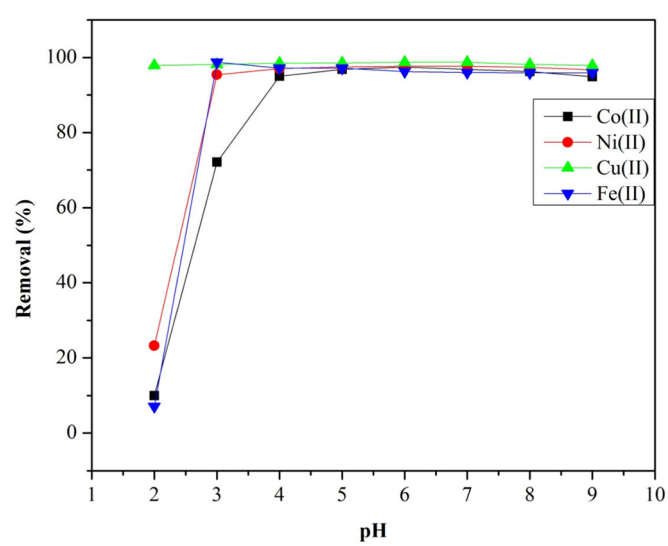

Fig. 6. Effect of pH on the adsorption of 20 mg/L of cobalt, copper, iron and nickel ions from an aqueous solution onto MCFs.

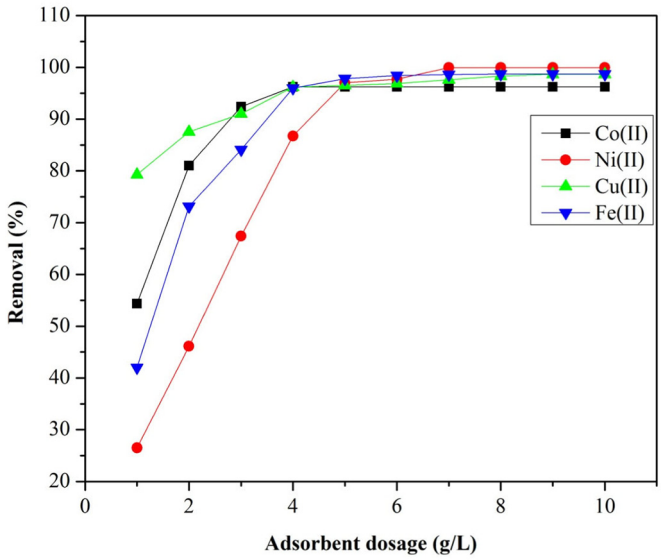

Fig. 7. Effect of dosage on the adsorption of 20 mg/ L of cobalt, copper, iron and nickel from an aqueous solution onto MCFs.

that metal ion removal efficiency considerably increased with time. The adsorption equilibrium was determinedas 60 min for copper, 40 min for iron, 24 min for nickel and 12 min for cobalt. During this short contact time, the elimination efficiency rapidly increased, due to the large surface area of MCFs. The adsorption process was constant after equilibrium since the adsorbent surface was almost completely used by the metal ions, and the increase of electrostatic repulsion between incoming metal ions and adsorbed metal ions.

Adsorption kinetics describes the solute adsorption rate. This rate controls the residence time of adsorbate uptake at the solid-liquid interface. In order to determine the rate-controlling step of heavy metal ions removal, pseudo-first-order, pseudo-second-order, intra-particle diffusion and Elovich models were fit to the experimental data. The Lagergren pseudo-first-order equation is written as:

$$\log(q_e - q_t) = \log q_e - \frac{k_1}{2.303}t \tag{3}$$

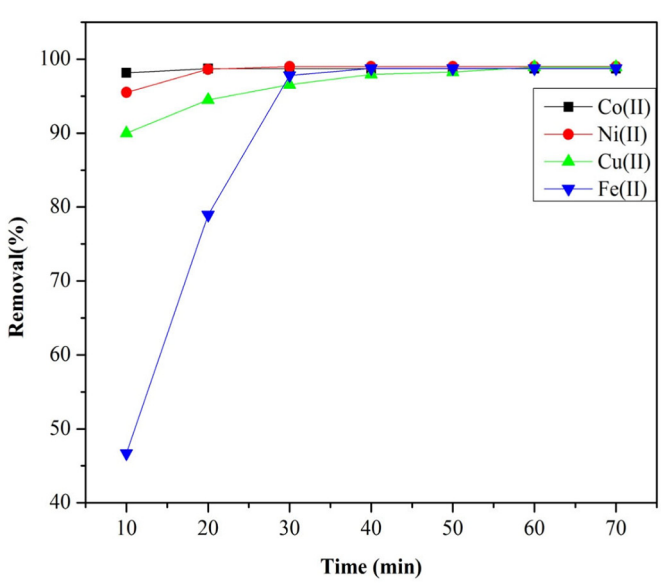

Fig. 8. Effect of contact time on the adsorption of cobalt, copper, iron and nickel ions onto MCFs at initial metal ion concentrations of 20 mg/ L and 30 °C.

Ho pseudo-second-order equation can be written as:

$$\frac{t}{q_t} = \frac{1}{k_2 q_e^2} + \frac{t}{q_e} \tag{4}$$

where q_e (mg/g) is the adsorption capacity of metal ions at equilibrium, q_t (mg/g) is the adsorption capacity at time t (min), k_1 (min^{-1}) and k_2 (g mg^{-1} min^{-1}) are the rate constant of first order kinetics and second-order, respectively. For the pseudo-first order kinetic model, k_1 and q_e can be calculated from the slope and intercept of the linear plot of log (q_e – q_t) versus t, respectively (Fig. S4). For the pseudo-second order kinetic model, k_2 and q_e values can be obtained from the intercept and slope of the plot of t/ q_t versus t, respectively (Fig. 9).

In order to determine the kinetic model that best described the adsorption process of the heavy metal ions, three criteria were used, namely, regression coefficients (R^2), predicted q_e values and Chi-square (χ^2) test. Data analysis is often performed by linear regression and model fitting is estimated based on the value of the regression coefficients (R^2). However, in some cases R^2 is not suitable and the Chi-square statistics test is used to determine the best kinetic model. This test is the sum of the squares of the differences between the experimental values and the data predicted by the kinetic models. The mathematical expression of the Chi-square (χ^2) is given by:

$$\chi^2 = \sum \frac{\left(q_{e(\,exp.)} - q_{e(cal.)}\right)^2}{q_{e(cal.)}} \tag{5}$$

where $q_{e(cal.)}$ and $q_{e(exp.)}$ are the equilibrium capacity (mg/g) calculated from the kinetic model (cal.) and experimental (exp.) data, respectively.

Comparing the results of the pseudo-second order with those of the pseudo-first-order kinetic models (Table 1), it can be seen that, the values of $q_{e(cal)}$ were more similar to those of $q_{e(exp)}$, the Chi-square (χ^2) test results were lower and the regression coefficients (R^2) were larger ($R^2 > 0.99$) for the former than for the latter. This showed that the experimental data can be nicely described by the pseudo-second order kinetic model. The results also suggest that chemisorption is taking place, which can be a rate limiting step in the metal ion adsorption process.

Weber and Morris equation can be written as:

$$q_t = k_{id} t^{1/2} + C \tag{6}$$

where, k_{id} is the intra-particle diffusion rate constant (mg/g $min^{1/2}$), the C constant is the intercept which indicates that the thickness of molecule boundary layer can also be obtained from the slope and intercept of the plots of q_t versus $t^{1/2}$, respectively (Fig. S5). The higher intercept value shows the larger boundary layer effect. As can be seen in Table 2, the values of C are high for all metals, which indicate that the surface biosorption has a good impact in the rate-controlling step [43]. As shown in Fig. S5 the intra-particle diffusion process takes place in two steps, with one break point. At the first stage, which is the fastest step, diffusion of metal ions through the aqueous solution takes place, at the external surface of MCFs or the boundary layer diffusion of the adsorbate molecules [44]. In the second stage, metal ions enter into the pores by intra-particle diffusion; this process is slow leading to equilibrium. Generally, if the first sharper section passes through the origin, the intra-particle diffusion is the rate-controlling step. But if the linear fitting plot does not pass through the origin, then there is an initial boundary layer resistance and the intra-particle diffusion is not the rate-governing step. As can be seen in Fig. S5, the linear fitting plots do not pass through the origin, showing that the intra-particle diffusion is involved in the adsorption process, but it is not the sole rate-limiting step for adsorption of heavy metal ions onto MCFs.

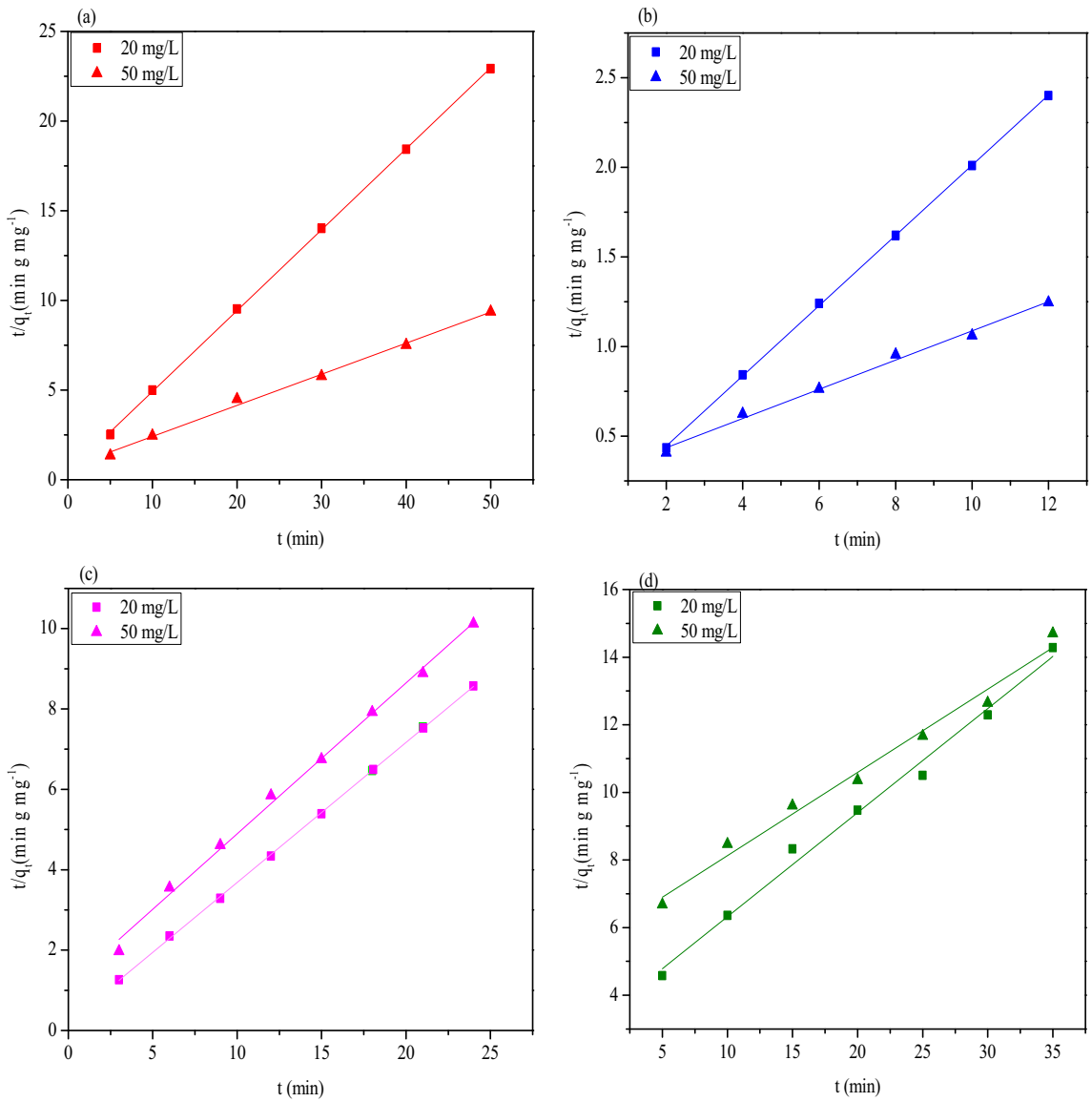

Fig. 9. Pseudo second order kinetic plots for the adsorption of (a) Cu(II) (b) Co(II), (c) Ni(II) and (d) Fe(II) for initial metal ion concentrations of 20 and 50 mg/ L.

The linear form of the Elovich equation is given as:

$$q_t = \frac{1}{\beta}\ \ln(\alpha\beta) + \frac{1}{\beta}\ln t \tag{7}$$

where α is the Elovich initial adsorption rate constant (mg/ g min^{-1}) and β is related to the extent of surface coverage and chemisorption activation energy (g mg^{-1}). The Elovich parameters α and β can be calculated from the slope and intercept of the linear plot of q_t versus lnt, respectively (Fig. S6). The Elovich equation is used to explain the second

Table 1
Pseudo-first-order and pseudo-second-order kinetic parameters for the adsorption of Co(II), Cu(II), Ni(II), and Fe(II) metal ions on MCFs for an initial concentration of 20 and 50 mg/ L.

Metal ions	C_0 (mg/L)	q_e(exp) (mg/g)	Pseudo-first- order				Pseudo-second order			
			k_1 (min^{-1})	q_e (mg/g)	R^2	χ^2	k_2 (g mg^{-1} min^{-1})	q_e (mg/g)	R^2	χ^2
Cu(II)	20	2.19	0.069	2.92	0.988	1.58	0.510	2.21	0.999	0.05
	50	5.34	0.122	5.79	0.827	1.77	0.043	5.78	0.995	1.75
Co(II)	20	4.99	0.379	1.14	0.956	84.95	0.757	5.10	0.999	0.10
	50	9.65	0.506	25.76	0.855	86.03	0.024	12.34	0.993	12.05
Ni(II)	20	2.81	0.181	1.70	0.949	4.09	0.577	2.88	0.999	0.14
	50	2.38	0.211	2.73	0.923	1.62	0.124	2.66	0.996	1.38
Fe(II)	20	2.46	0.172	5.66	0.943	18.81	0.029	3.24	0.991	4.07
	50	2.39	0.175	7.88	0.886	37.37	0.010	4.06	0.985	10.34

Table 2
Intra-particle diffusion model and Elovich kinetic model parameters for the adsorption of Co(II), Cu(II), Ni(II), and Fe(II) metal ions by MCFs for an initial concentration of 20 and 50 mg/ L.

Metal ions	C_0 (mg/L)	Intraparticle diffusion model			Elovich model		
		k_{id} (mg/gmin^{-1})	C (mg/g)	R^2	α	β	R^2
Cu(II)	20	0.044	1.886	0.958	1.820	0.092	0.952
	50	0.373	2.877	0.952	2.316	0.789	0.951
Co(II)	20	0.194	4.339	0.978	4.433	0.225	0.992
	50	2.378	1.703	0.983	2.870	2.735	0.988
Ni(II)	20	0.136	2.224	0.787	2.170	0.221	0.899
	50	0.283	1.050	0.968	0.999	0.432	0.975
Fe(II)	20	0.388	0.305	0.966	0.137	0.748	0.983
	50	0.473	0.276	0.984	0.783	0.900	0.983

order kinetics and assumes that the solid surface of the MCFs is heterogeneous. The values of parameters of Elovich model for all heavy metal ions are given in Table 2.

Residual plots of kinetics models are graphics that show the residuals on the vertical axis and the independent variable (q_e predicted value) on the horizontal axis. If the points in residual plots are randomly dispersed around the horizontal axis, a linear regression model is appropriate for the data; otherwise, a non-linear model is more appropriate. The residual plots of pseudo-first order and pseudo-second order kinetic models are shown in Figs. S7–S10.

3.5. Effect of concentration and adsorption isotherms

The influence of the initial concentration (varying from 5 to 50 mg/L) on the adsorption of heavy metal ions (Cu^{2+}, Ni^{2+}, Co^{2+} and Fe^{2+}) was determined at 30 °C. To explain the removal mechanism, two adsorption isotherms models namely, Langmuir and Freundlich, were plotted to fit the experimental data. The calculated parameters are listed in Table 3.The Langmuir isotherm is described by the equation:

$$q_e = \frac{q_m K_L C_e}{1 + K_L C_e} \tag{8}$$

The Freundlich isotherm is characterized by the equation:

$$\log q_e = \log K_F + \frac{1}{n} \log C_e \tag{9}$$

where q_e (mg/g) is the adsorption capacity of metal ions at equilibrium, C_e (mg/L) is the equilibrium concentration of metal ions in solution, q_m (mg/g) is the maximum adsorption capacity of metal ion, K_L (L/g) is a Langmuir model constant. K_F and n are Freundlich model constants. The plots of Langmuir and Freundlich models are shown in Fig. 10. Moreover, another parameter of the Langmuir isotherm, the dimensionless separation factor R_L, can be used for evaluation. It can be calculated by the equation [45]:

Table 3
Langmuir and Freundlich model constants and coefficients for adsorption of Cu(II), Ni(II), Co(II) and Fe(II) onto MCFs at 30 °C.

Metal ions	Langmuir isotherm				Freundlich isotherm		
	q_m (mg/g)	K_L	R_L	R^2	K_f (mg/g) (mg/L)^n	n	R^2
Cu(II)	200.0	0.016	0.757	0.976	4.03	1.12	0.948
Co(II)	50.0	0.085	0.369	0.977	190.55	5.15	0.875
Ni(II)	4.85	6.87	0.007	0.998	128.82	5.05	0.784
Fe(II)	43.47	0.075	0.4	0.984	3.66	1.12	0.979

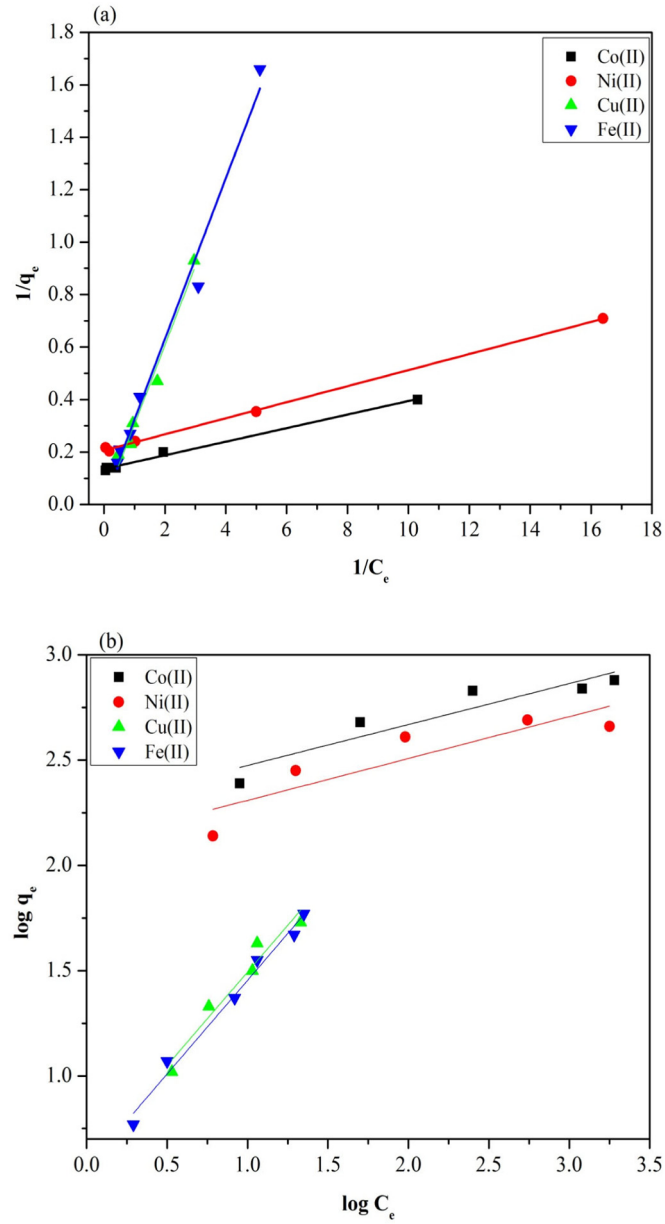

Fig. 10. (a) Langmuir and (b) Freundlich adsorption isotherm fitting on Cu^{2+}, Ni^{2+}, Co^{2+} and Fe^{2+} ions.

$$R_L = \frac{1}{1 + K_L C_0} \tag{10}$$

where C_0 is the initial concentration of metal ions. The R_L value shows that the isotherm and the adsorption process are unfavourable (if $R_L > 1$), linear (if $R_L = 1$), favourable (if $0 < R_L < 1$) or irreversible (if $R_L = 0$). In this work, the calculated R_L values indicate that metal ions adsorption on MCFs was favourable.

Table 3 shows that the R^2 values for the Langmuir isotherm were higher than those of the Freundlich model. Hence, the Langmuir model can better fit the data of adsorption equilibrium. Thus, it can be concluded that homogeneous and monolayer coverage of Cu^{2+}, Ni^{2+}, Co^{2+} and Fe^{2+} takes place on the surface of MCFs. According to the model of Langmuir, the maximum adsorption capacities (Q_{max}) for Cu^{2+}, Ni^{2+}, Co^{2+} and Fe^{2+} ions were estimated to be 200.0, 4.85, 50.0 and 43.47 mg/g, respectively, which are higher than other adsorbents

derived from CFs reported in the literature, as will be seen in Section 3.10.

3.6. Effect of temperature and adsorption thermodynamics

The thermodynamic parameters were obtained from the Van't Hoff equation and are shown in Table 4. The standard enthalpy (ΔH^0) and standard entropy (ΔS^0) values were obtained from the slope and intercept of Eq. (9), respectively (Fig. 11).

$$\ln K_d = \frac{\Delta S^0}{R} - \frac{\Delta H^0}{RT} \tag{11}$$

where R is the universal gas constant(8.314 J/mol K), T is the absolute temperature (in K), K_d is a thermodynamic equilibrium constant, defined by:

$$K_d = \frac{C_A}{C_B} \tag{12}$$

where C_A and C_B are, respectively, the concentration on the adsorbate and on the adsorbent and residual concentration at equilibrium. The value of Gibbs free energy (ΔG^0) can be obtained from Eq. (11) at 30–50 °C. The negative values of ΔG^0demonstrate that adsorption of Cu^{2+}, Ni^{2+}, Co^{2+} and Fe^{2+} ions onto MCFs is spontaneous.

$$\Delta G^0 = -RT\ln K_d \tag{13}$$

The positive values of ΔH^0 for all metal ions demonstrate that the adsorption process is endothermic. Also, the positive values of ΔS^0confirmed that the solid– liquid interface has larger randomness, when adsorption is taking place.

3.7. Metal adsorption selectivity

Adsorption of the heavy metal ions onto MCFs could be explained by the Pearson's theory, which states that the Cu(II), Ni(II), Co(II) and Fe(II) ions can be considered borderline Lewis acids, whereas the hydroxyl ion is considered as a hard Lewis base. Therefore, hard acids are more likely to bind with hard bases [46]. The adsorption preference of the adsorbent for Cu(II) can also be due to its largest atomic weight (63.54), paramagnetic behaviour ($3d^9 4s^2$), largest electronegativity (1.95), smaller ionic radius (0.69), and higher standard reduction potential (0.34 V), compared to Ni(II), Co(II) and Fe(II) ions to result in easy adsorption on MCFs with the highest adsorption capacity [47]. There are many factors that affect the adsorption process, such as electronegativity, ionic radius, standard reduction potential, already mentioned, but also the position in the Irving-Williams series and other ionic properties are the main reasons for the difference in metal adsorption capacity [48]. Another reason can be related to the John-Teller Effect, which is predominant for the copper complex, compared to other metal ions [49].

3.8. Adsorption mechanism

FTIR spectra of MCFs with metal ions (Fig. 2) show that peaks at 3438, 1641, 1241 and 1062 cm^{-1} have distinct changes after the metal ions were adsorbed. These results indicated that the hydroxyl, carboxylate and amino groups are involved in the adsorption process [47].

The elemental composition of different elements on the surface of the modified and metal ions loaded MCFs are shown in Fig. 4. The EDX spectra of MCFs show that sodium was introduced onto the adsorbent surface in the modification process by using the sodium hydroxide to neutralize the carboxyl groups. When the adsorption process occurred, Na^+ was replaced by Cu^{2+}, Ni^{2+}, Co^{2+} and Fe^{2+}. The schematic representation of possible mechanism of adsorption of metal ions by MCFs is shown in Fig. 12

Table 4
Thermodynamic parameters for adsorption of Cu(II), Ni(II), Co(II) and Fe(II) onto MCFs.

Metal ions	C_0 (mg/L)	ΔH^0 (KJ/mol)	ΔS^0(J/mol/K)	ΔG^0 (KJ/mol)		
				303 K	313 K	323 K
Cu(II)	20	4.57	44.25	−8.84	−9.26	−9.72
Co(II)	20	4.57	49.05	−10.27	−10.79	−11.25
Ni(II)	20	19.12	100.93	−11.56	−12.28	−13.56
Fe(II)	20	4.15	41.48	−8.41	−8.82	−9.23

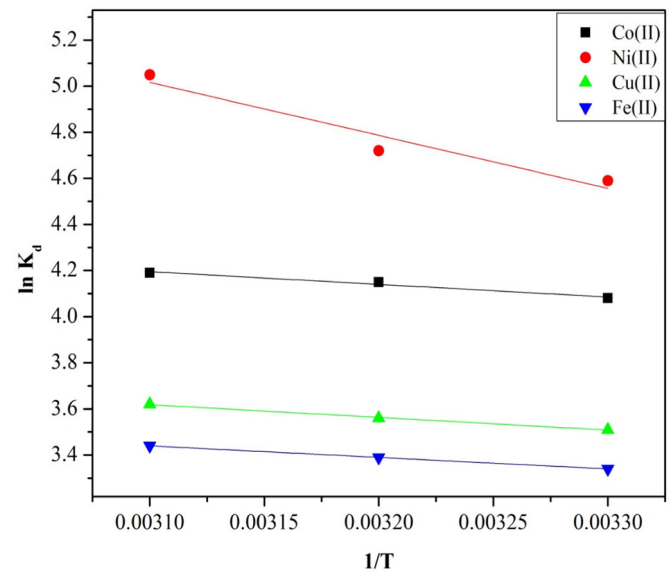

Fig. 11. Van't Hoff's plot for the determination of the thermodynamic parameters for removal of Cu(II), Ni(II), Co(II) and Fe(II) onto MCFs.

3.9. Desorption

The regeneration of the adsorbent is a very important parameter and can be carried out by batch method. Therefore, the desorption performance of MCFs was also investigated. An EDTA solution (0.1 M) was used as the eluting agent for metal ion desorption. As shown in (Fig. 13), the regeneration efficiencies for Co(II), Cu(II), Fe(II) and Ni (II) adsorption were 90.7%, 89.8%, 89.2% and 96.6%, respectively, after 7 cycles, with a relatively low decrease, revealing the excellent reusability and stability of the MCFs.

3.10. Comparison with other adsorbents

The maximum removal capacities of various literature reported (low-cost) adsorbents are compared with MCFs in Table 5. It can be seen that the MCFs can adsorb a larger amount of metal ions from aqueous solutions, compared to other materials. Thus, this low-cost adsorbent has great potential for metal ion removal.

Table 6 also compares the reported maximum adsorption capacities of chemically modified chicken feathers for other heavy metal ions removal, in order to show the potential application of MCFs materials. Other authors tried to chemically treat chicken feathers for removal of heavy metal ions, such as Cr(VI) and As(III) with interesting results, especially for Cr(VI) removal using alkali treated CFs [58]. Nevertheless, better results were obtained with Cu(II) in our present work (as seen in Table 5).

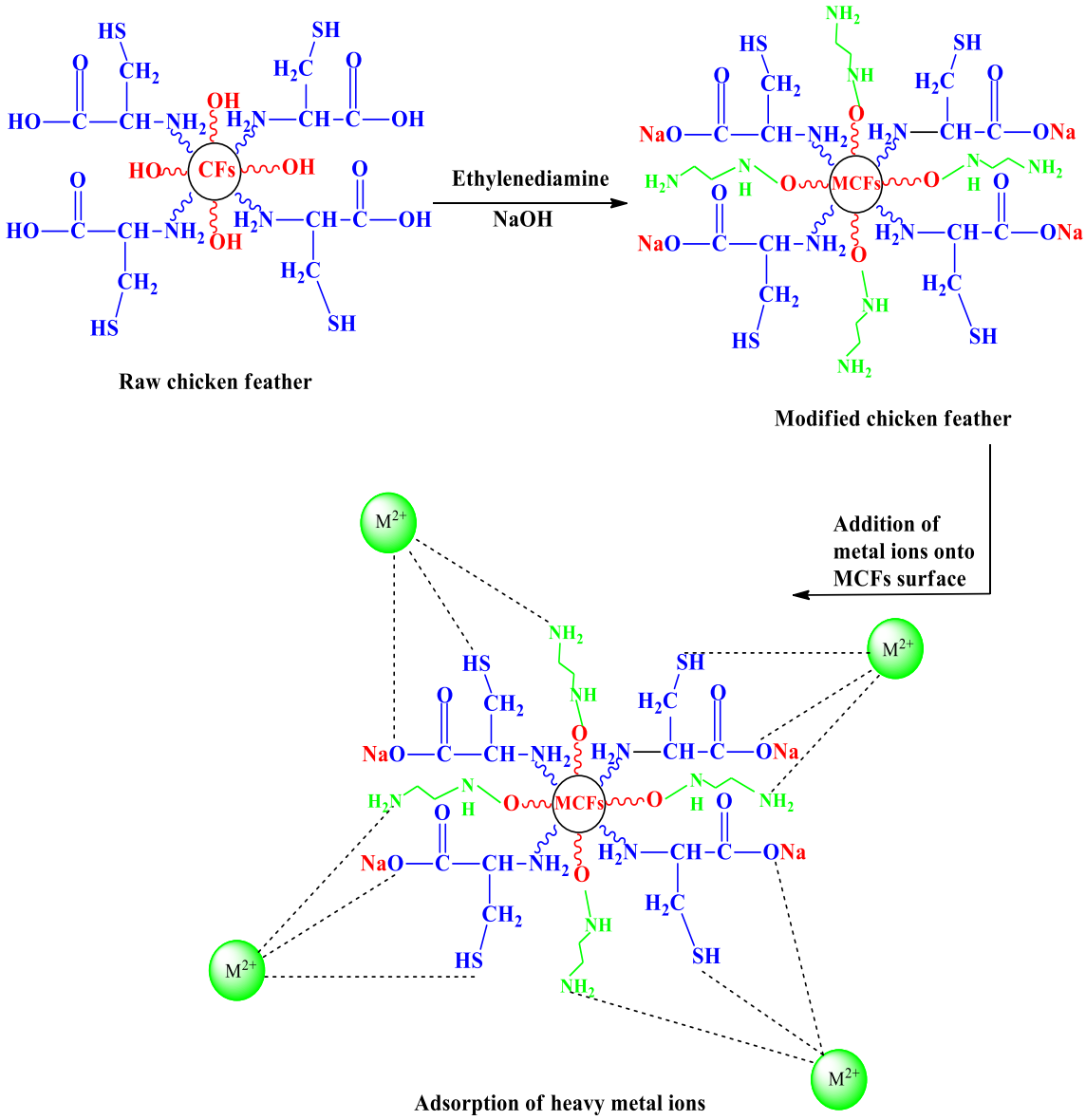

Fig. 12. The proposed adsorption mechanism of Cu(II), Ni(II), Co(II) and Fe(II) metal ions as M^{2+} onto MCFs.

4. Conclusions

In this work, MCFs were used to test the adsorption of the heavy metal ions Cu(II), Ni(II), Co(II) and Fe(II), from aqueous solutions, under different conditions: adsorbent concentration, pH and time. The FTIR and SEM-EDX analysis evidenced that metal ions were successfully loaded on the surface of MCFs. The maximum adsorption capacities were 200.0, 50.0, 43.47, and 4.85 mg/g, respectively, following the sequence: Cu(II) > Co (II) > Fe(II) > Ni(II). Removal efficiencies of Co(II), Cu(II), Fe(II) and Ni (II) ions were 98.9%, 98.7%, 98.7% and 99%, respectively, for an initial concentration of 20 mg/L. The adsorption isotherms were well explained by the Langmuir isotherm model. Removal of metal ions by MCFs was described by a pseudo-second-order chemisorption model. The adsorption process of metal ions by MCFs was endothermic and spontaneous, as shown by the thermodynamic calculations. MCFs exhibited a good recyclability and large adsorption efficiency even after 7 cycles of use.

CRediT authorship contribution statement

Rupa Chakraborty: Data curation, Formal analysis, Investigation, Resources, Software, Writing - original draft, Writing - review & editing, Methodology.**Anupama Asthana:**Conceptualization, Supervision.**Ajaya Kumar Singh:**Funding acquisition, Project administration, Resources, Software, Writing - review & editing.**Sushma Yadav:**Visualization.**Md. Abu Bin Hasan Susan:**Validation, Writing - original draft, Writing - review & editing.**Sónia A.C. Carabineiro:**Funding acquisition, Writing - review & editing.

Declaration of competing interest

There are no conflicts to declare.

Acknowledgements

Authors are thankful to SAIF centre STIC Kochi (Keral) and NIT Raipur (Chhattisgarh) for providing instrumental facilities and to lab staff and research scholars at Department of Chemistry, Govt. V.Y.T. PG. Autonomous College, Durg, (C.G.), India for their support. This work has also been supported by the Associate Laboratory for Green Chemistry —LAQV, financed by national funds from FCT/MCTES (UIDB/50006/2020).

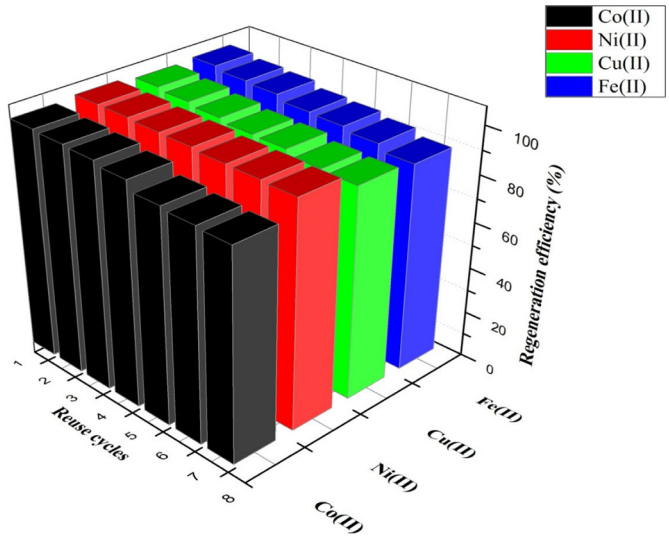

Fig. 13. Adsorption capacities of Cu(II), Ni(II) and Co(II)onto MCFs up to seven adsorption–desorption cycles.

Table 5
Comparison of maximum adsorption capacities for different adsorbents reported in literature.

S. no.	Adsorbent materials	Adsorption capacity (mg/g)				References
		Cu(II)	Ni(II)	Co(II)	Fe(II)	
1.	Wheat straw	5	2.5	–	–	[50]
2.	Modified jute fibres	7.73	5.57	–	–	[51]
3.	Alkali-treated lemon peel	–	–	35.71	–	[52]
4.	Kaolinite	10.787	1.669	0.919	–	[53]
5.	Wooden charcoal	–	–	–	1.234	[54]
6.	Modified barley straw	31.71	–	–	–	[55]
7.	Cashew nut shell	–	18.868	–	–	[56]
8.	Modified chicken feathers	200.0	4.85	50.0	43.47	This work

Table 6
Comparison of maximum adsorption capacities of chemically modified chicken feathers for different heavy metal ions removal reported in literature.

S. no.	Adsorbent	Metal ions	Adsorption capacity (mg/g)	References
1.	EAEpi-chicken feather	Cr(VI)	14.47	[57]
2.	Alkali-treated chicken feather	Cr(VI)	90.91	[58]
3.	Allyl alcohol treated chicken feather	As (III)	11.5×10^{-2}	[59]
4.	TrisilanolCyclohexyl treated chicken feather	As (III)	11.0×10^{-2}	[59]

Appendix A. Supplementary data

Supplementary data to this article can be found online at https://doi.org/10.1016/j.molliq.2020.113475.

References

[1] A.A. Ismaiel, M.K. Aroua, R. Yusoff, Palm shell activated carbon impregnated with task-specific ionic-liquids as a novel adsorbent for the removal of mercury from contaminated water, Chem. Eng. J. 225 (2013) 306–314, https://doi.org/10.1016/j.cej.2013.03.082.

[2] S. Siva, S. Sudharsan, R.S. Kannan, Synthesis, characterization and ion exchange properties of novel hybrid polymer nanocomposites for selective and effective mercury (II) removal, RSC Adv. 5 (2015) 79665–79678, https://doi.org/10.1039/C5RA13004B.

[3] R. Laus, T.G. Costa, B. Szpoganicz, V.T. Favere, Adsorption and desorption of cu(II) and Pb(II) ions using chitosan cross linked with epichlorohydrin triphosphate as the adsorbent, J. Hazard. Mater. 183 (2010) 233–241, https://doi.org/10.1016/j.jhazmat.2010.07.016.

[4] S. Rengaraj, Y. Kim, C.K. Joo, J. Yi, Removal of copper from aqueous solution by aminated and protonated mesoporousaluminas: kinetics and equilibrium, J. Colloid Interface Sci. 273 (2004) 14–21, https://doi.org/10.1016/j.jcis.2004.01.007.

[5] A. Ahmad, M. Rafatullah, O. Sulaiman, M.H. Ibrahim, Y.Y. Chii, B.M. Siddique, Removal of Cu(II) and Pb(II) ions from aqueous solutions by adsorption on sawdust of Meranti wood, Desalination 247 (2009) 636–646, https://doi.org/10.1016/j.desal.2009.01.007.

[6] F.L. Mi, S.J. Wu, F.M. Lin, Adsorption of copper(II) ions by a chitosan–oxalatecomplex biosorbent, Int. J. Biol. Macromol. 72 (2015) 136–144, https://doi.org/10.1016/j.ijbiomac.2014.08.006.

[7] R. Verma, A. Asthana, A.K. Singh, S. Prasad, An arginine functionalized magnetic nano-sorbentfor simultaneous removal of three metal ions from water samples, RSC Adv. 7 (2017) 51079–51089, https://doi.org/10.1039/C7RA09705K.

[8] A. Bhatnagar, A.K. Minocha, M. Sillanpaa, Adsorptive removal of cobalt from aqueous solution by utilizing lemon peel as biosorbent, Biochem. Eng. J. 48 (2010) 181–186, https://doi.org/10.1016/j.bej.2009.10.005.

[9] A. Asthana, R. Verma, A.K. Singh, M.A.B.H. Susan, R. Adhikari, Silver nanoparticle entrapped calcium alginate beads for Fe(II) removal via adsorption, Macromol. Symp. 366 (2016) 42–51, https://doi.org/10.1002/masy.201650045.

[10] V.C. Srivastava, I.D. Mall, I.M. Mishra, Competitive adsorption of cadmium(II) and nickel(II) metal ions fromaqueous solution onto rice husk ash, Chem. Eng. Process. 48 (2009) 370–379, https://doi.org/10.1016/j.cep.2008.05.001.

[11] Y. Hannachi, N.A. Shapovalov, A. Hannachi, Adsorption of nickel from aqueoussolution by the use of low-cost adsorbents, Korean J. Chem. Eng. 27 (2010) 152–158, https://doi.org/10.1007/s11814-009-0303-7.

[12] S. Rengaraj, C.K. Joo, Y. Kim, J. Yi, Kinetics of removal of chromium from water and electronic process wastewater by ion exchange resins: 1200H, 1500H andIRN97H, J. Hazard. Mater. 102 (2003) 257–275, https://doi.org/10.1016/s0304-3894(03)00209-7.

[13] M. Uysal, A. Irfan, Removal of Cr(VI) from industrial wastewaters by adsorption part I: determination of optimum condition, J. Hazard. Mater. 149 (2007) 482–491, https://doi.org/10.1016/j.jhazmat.2007.04.019.

[14] C. Li, H. Chen, Z. Li, Adsorptive removal of Cr(VI) by Fe-modified steam exploded wheat straw, Process Biochem. 39 (2004) 541–545, https://doi.org/10.1016/s0032-9592(03)00087-6.

[15] M. Jain, V.K. Garg, K. Kadirvelu, Adsorption of hexavalent chromium from aqueous medium onto carbonaceous adsorbents prepared from waste biomass, J. Environ. Manag. 91 (2010) 949–957, https://doi.org/10.1016/j.jenvman.2009.12.002.

[16] S.A.C. Carabineiro, T. Thavorn-amornsri, M.F.R. Pereira, J.L. Figueiredo, Adsorption of ciprofloxacin on surface-modified carbon materials, Water Res. 45 (2011) 4583–4591, https://doi.org/10.1016/j.watres.2011.06.008.

[17] S.A.C. Carabineiro, T. Thavorn-amornsri, M.F.R. Pereira, P. Serp, J.L. Figueiredo, Comparison between activated carbon, carbon xerogel and carbon nanotubes for the adsorption of the antibiotic ciprofloxacin, Catal. Today 186 (2012) 29–34, https://doi.org/10.1016/j.cattod.2011.08.020.

[18] A. Hashmi, A.K. Singh, B. Jain, S.A.C. Carabineiro, Chloramine-T/N bromosuccinimide/$FeCl_3$/KIO_3decorated graphene oxide nanosheets and their antibacterial activity, Nanomaterials 10 (2020) 105, https://doi.org/10.3390/nano10010105.

[19] A. Hashmi, A.K. Singh, B. Jain, A. Singh, Muffle atmosphere promoted fabrication of graphene oxide nanoparticle by agricultural waste, Fullerenes, Nanotubes, Carbon Nanostruct, 2020https://doi.org/10.1080/1536383X.2020.1728744 , (In press).

[20] S. Yadav, A. Asthana, R. Chakraborty, B. Jain, A.K. Singh, S.A.C. Carabineiro, M.A.B.H. Susan, Cationic dye removal using novel magnetic/activated charcoal/β-cyclodextrin/alginate polymer nanocomposite, Nanomaterials 10 (2020) 170, https://doi.org/10.3390/nano10010170.

[21] R. Chakraborty, A. Asthana, A.K. Singh, B. Jain, M.A.B.H. Susan, Adsorption of heavy metal ions by various low cost adsorbents: a review, Int. J. Environ. Anal. Chem. (2020)https://doi.org/10.1080/03067319.2020.1722811.

[22] H. Lin, S. Han, Y. Dong, Y. He, The surface characteristics of hyperbranched polyamide modifiedcorncob and its adsorption property for Cr(VI), Appl. Surf. Sci. 412 (2017) 152–159, https://doi.org/10.1016/j.apsusc.2017.03.061.

[23] T.D. Šoštarić, M.S. Petrović, F.T. Pastor, D.R. Lončarević, J.T. Petrović, J.V. Milojković, M.D. Stojanovi, Study of heavy metals biosorption on native and alkali treated apricot shells and its application in wastewater treatment, J. Mol. Liq. 259 (2018) 340–349, https://doi.org/10.1016/j.molliq.2018.03.055.

[24] I. Ullah, R. Nadeem, M. Iqbal, Q. Manzoor, Biosorption of chromium onto native and immobilized sugarcane bagasse waste biomass, Ecol. Eng. 60 (2013) 99–107, https://doi.org/10.1016/j.ecoleng.2013.07.028.

[25] R. Chakraborty, R. Verma, A. Asthana, S. Sree Vidya, A.K. Singh, Adsorption of hazardous chromium (VI) ions from aqueous solutions using modified sawdust: kinetics, isotherm and thermodynamic modelling, Int. J. Environ. Anal. Chem. (2019) https://doi.org/10.1080/03067319.2019.1673743.

[26] Y. Yi, J. Lv, Y. Liu, G. Wu, Synthesis and application of modified Litchi peel for removal of hexavalent chromium from aqueous solutions, J. Mol. Liq. 225 (2017) 28–33, https://doi.org/10.1016/j.molliq.2016.10.140.

[27] S. Rangabhashiyam, N. Selvaraju, Adsorptive remediation of hexavalent chromium from synthetic wastewater by a natural and ZnCl2 activated Sterculia guttata shell, J. Mol. Liq. 207 (2015) 39–49, https://doi.org/10.1016/j.molliq.2015.03.018.

[28] S. Rangabhashiyam, N. Selvaraju, Efficacy of unmodified and chemically modified Swieteniamahagoni shells for the removal of hexavalent chromium from simulated wastewater, J. Mol. Liq. 209 (2015) 487–497, https://doi.org/10.1016/j.molliq.2015.06.033.

[29] S. Doyurum, A. Celik, Pb(II) and cd(II) removal from aqueous solutions by olive cake, J. Hazard. Mater. B 138 (2006) 22–28, https://doi.org/10.1016/j.jhazmat.2006.03.071.
[30] K.M. Arai, R. Takahashi, Y. Yokote, K. Akahane, Amino-acid sequence of feather keratin from fowl, Eur. J. Biochem. 132 (1983) 501–507, https://doi.org/10.1111/j.1432-1033.1983.tb07389.x.
[31] S. Al-Asheh, F. Banat, D. Al-Rousan, Beneficial reuse of chicken feathers in removal of heavy metals from wastewater, J. Clean. Prod. 11 (2003) 321–326, https://doi.org/10.1016/S0959-6526(02)00045-8.
[32] A. Mittal, Use of hen feathers as potential adsorbent for the removal of a hazardous dye, brilliant blue FCF, from wastewater, J. Hazard. Mater. B 128 (2006) 233–239, https://doi.org/10.1016/j.jhazmat.2005.08.043.
[33] W. Fresenius, K.E. Quentin, W. Schneider, Water Analysis: A Practical Guide to Physico-Chemical, Chemical and Microbiological Water Examination and Quality Assurance, 373, Springer Science & Business Media, 1988 1–804.
[34] P. Gao, Z. Liu, X. Wu, Z. Cao, Y. Zhuang, W. Sun, G. Xue, M. Zhou, Biosorption of chromium(VI) ions by deposits produced from chicken feathers after soluble keratin extraction, Clean – Soil, Air, Water 42 (2014) 1558–1566, https://doi.org/10.1002/clen.201300669.
[35] A. Vasconcelos, G. Freddi, A. Cavaco-Paulo, Biodegradable materials based on silk fibroin and keratin, Biomacromolecules 9 (2008) 1299–1305, https://doi.org/10.1021/bm7012789.
[36] H. Qiu, J. Yan, G. Lan, Y. Liu, X. Song, W. Peng, Y. Cui, Removal of Cu^{2+} from wastewater by modified xanthan gum (XG) with ethylenediamine (EDA), RSC Adv. 6 (2016) 83226–83233, https://doi.org/10.1039/C6RA11423G.
[37] E. Menefee, G. Yee, Thermally-induced structural changes in wool, Text. Res. J. 35 (1965) 801–812, https://doi.org/10.1177/004051756503500904.
[38] P. Milczarek, M. Zielinski, M. Garcia, The mechanism and stability of thermal transitions in hair keratin, Colloid Polym. Sci. 270 (1992) 1106–1115, https://doi.org/10.1007/BF00652875.
[39] F. Wortmann, M. Stapels, R. Elliott, L. Chandra, The effect of water on the glass transition of a human hair, Biopolymers 81 (2006) 371–375, https://doi.org/10.1002/bip.20429.
[40] T. Tesfaye, B. Sithole, D. Ramjugernath, T. Mokhothu, Valorisation of chicken feathers: characterisation of thermal, mechanicaland electrical properties, Sustain. Chem. Pharm. 9 (2018) 27–34, https://doi.org/10.1016/10.1016/j.scp.2018.05.003.
[41] P.S. Kumar, S. Ramalingam, V. Sathyaselvabala, S.D. Kirupha, A. Murugesan, S. Sivanesan, Removal of cadmium(II) from aqueous solutionby agricultural waste cashew nut shell, Korean J. Chem. Eng. 29 (2012) 756–768, https://doi.org/10.1007/s11814-011-0259-2.
[42] S. Liang, N. Ye, Y. Hu, Y. Shi, W. Zhang, W. Yu, X. Wu, J. Yang, Lead adsorption from aqueous solutions by a granular adsorbent prepared from phoenix tree leaves, RSC Adv. 6 (2016) 25393–25400, https://doi.org/10.1039/C6RA03258C.
[43] A.E. Ofomaja, E.B. Naidoo, S.J. Modise, Kinetic and pseudo-second-order modelling of lead biosorption onto pine cone powder, Ind. Eng. Chem. Res. 49 (2010) 2562–2572.
[44] R.M. Ali, H.A. Hamad, M.M. Hussein, G.F. Malash, Potential of using green adsorbent of heavy metal removal from aqueous solutions: adsorption kinetics, isotherm, thermodynamic, mechanism and economic analysis, Ecol. Eng. 91 (2016) 317–332, https://doi.org/10.1016/j.ecoleng.2016.03.015.
[45] H. Gupta, P.R. Gogate, Intensified removal of copper from waste water using activated watermelon based biosorbent in the presence of ultrasound, Ultrason. Sonochem. 30 (2016) 113–122, https://doi.org/10.1016/j.ultsonch.2015.11.016.
[46] S.N.C. Ramos, A.L.P. Xavier, F.S. Teodoro, L.F. Gil, L.V.A. Gurgel, Removal of cobalt(II), copper(II), and nickel(II) ions from aqueous solutions using phthalate-functionalized sugarcane bagasse: mono and multicomponent adsorption in batch mode, Ind. Crop. Prod. 79 (2016) 116–130, https://doi.org/10.1016/j.indcrop.2015.10.035.
[47] J. Yu, L. Wang, R. Chi, Y. Zhang, Z. Xu, J. Guo, Adsorption of Pb^{2+}, Cd^{2+}, Cu^{2+}, and Zn^{2+} from aqueous solution by modified sugarcane bagasse, Res. Chem. Intermed. 41 (2015) 1525–1541, https://doi.org/10.1007/s11164-013-1290-1.
[48] D. Ouyang, Y. Zhuo, L. Hu, Q. Zeng, Y. Hu, Z. He, Research on the adsorption behavior of heavy metal ions by porous material prepared with silicate tailings, Minerals 9 (2019) 291, https://doi.org/10.3390/min9050291.
[49] A. Ghaee, M. Shariaty-Niassar, J. Barzin, A. Zarghan, Adsorption of copper and nickel ions on macroporous chitosan membrane: equilibrium study, Appl. Surf. Sci. 258 (2012) 7732–7743, https://doi.org/10.1016/j.apsusc.2012.04.131.
[50] M. Gorgievski, D. Bozic, V. Stankovic, N. Strbac, S. Serbula, Kinetics, equilibrium and mechanism of Cu^{2+}, Ni^{2+} and Zn^{2+} ions biosorption using wheat straw, Ecol. Eng. 58 (2013) 113–122, https://doi.org/10.1016/j.ecoleng.2013.06.025.
[51] S.R. Shukla, R.S. Pai, Adsorption of Cu(II), Ni(II) and Zn(II) on modified jute fibres, Bioresour. Technol. 96 (2005) 1430–1438, https://doi.org/10.1016/j.biortech.2004.12.010.
[52] S.A. Singh, S.R. Shukla, Adsorptive removal of cobalt ions on raw and alkali-treated lemon peels, Int. J. Environ. Sci. Technol. 13 (2016) 165–178, https://doi.org/10.1007/s13762-015-0801-6.
[53] O. Yavuz, Y. Altunkaynak, F. Guzel, Removal of copper, nickel, cobalt and manganese from aqueous solution by kaolinite, Water Res. 37 (2003) 948–952, https://doi.org/10.1016/s0043-1354(02)00409-8.
[54] K.U. Ahmad, Md. Jawed, Kinetics, equilibrium and breakthrough studies for Fe(II) removal by wooden charcoal: a low-cost adsorbent, Desalination 251 (2010) 137–145, https://doi.org/10.1016/j.desal.2009.08.007.
[55] E. Pehlivan, T. Altun, S. Parlayici, Modified barley straw as a potential biosorbent for removal of copper ions from aqueous solution, Food Chem. 135 (2012) 2229–2234, https://doi.org/10.1016/j.foodchem.2012.07.017.
[56] P. Senthil Kumar, S. Ramalingam, S. Dinesh Kirupha, A. Murugesan, T. Vidhyadevi, S. Sivanesan, Adsorption behavior of nickel(II) onto cashew nut shell: Equilibrium, thermodynamics, kinetics, mechanism and process design, Chem. Eng. J. 167 (2011) 122–131, https://doi.org/10.1016/j.cej.2010.12.010.
[57] P. Sun, Z.T. Liu, Z.W. Liu, Chemically modified chicken feather as sorbent for removing toxic chromium(VI) ions, Ind. Eng. Chem. Res. 48 (2009) 6882–6889, https://doi.org/10.1021/ie900106h.
[58] N.K. Mondal, S. Basu, B. Das, Decontamination and optimization study of hexavalent chromium on modified chicken feather using response surface methodology, Appl Water Sci 9 (2019) 1–35, https://doi.org/10.1007/s13201-019-0930-z.
[59] M.A. Khosa, Aman Ullah, In-situ modification, regeneration, and application of keratin biopolymer for arsenic removal, J. Hazard. Mater. 278 (2014) 360–371, https://doi.org/10.1016/j.jhazmat.2014.06.023.